ACS APPLIED MATERIALS & INTERFACES

Research Article

Cite This: ACS Appl. Mater. Interfaces 2019, 11, 5492−5498

www.acsami.org

Ultrafast Zero-Bias Surface Photocurrent in Germanium Selenide: Promise for Terahertz Devices and Photovoltaics

Kateryna Kushnir,[†] Ying Qin,[‡] Yuxia Shen,[‡] Guangjiang Li,[†] Benjamin M. Fregoso,[§] Sefaattin Tongay,[‡] and Lyubov V. Titova*[,†]

[†]Department of Physics, Worcester Polytechnic Institute, Worcester, Massachusetts 01609, United States

[‡]School for Engineering of Matter, Transport and Energy, Arizona State University, Tempe, Arizona 85287, United States

[§]Department of Physics, Kent State University, Kent, Ohio 44242, United States

Supporting Information

ABSTRACT: Theory predicts that a large spontaneous electric polarization and concomitant inversion symmetry breaking in GeSe monolayers result in a strong shift current in response to their excitation in the visible range. Shift current is a coherent displacement of electron density on the order of a lattice constant upon above-bandgap photoexcitation. A second-order nonlinear effect, it is forbidden by the inversion symmetry in the bulk GeSe crystals. Here, we use terahertz (THz) emission spectroscopy to demonstrate that ultrafast photoexcitation with wavelengths straddling both edges of the visible spectrum, 400 and 800 nm, launches a shift current in the surface layer of a bulk GeSe crystal, where the inversion symmetry is broken. The direction of the surface shift current determined from the observed polarity of the emitted THz pulses depends only on the orientation of the sample and not on the linear polarization direction of the excitation. Strong absorption by the low-frequency infrared-active phonons in the bulk of GeSe limits the bandwidth and the amplitude of the emitted THz pulses. We predict that reducing GeSe thickness to a monolayer or a few layers will result in a highly efficient broadband THz emission. Experimental demonstration of THz emission by the surface shift current in bulk GeSe crystals puts this 2D material forward as a candidate for next-generation shift current photovoltaics, nonlinear photonic devices, and THz sources.

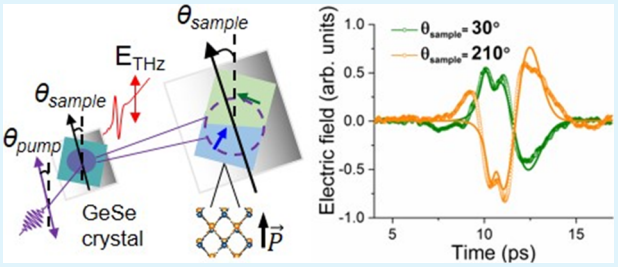

KEYWORDS: *GeSe, group-IV monochalcogenides, terahertz emission spectroscopy, shift current, bulk photovoltaic effect*

INTRODUCTION

Theoretical investigations of group-IV monochalcogenides indicate that monolayer GeS, GeSe, SnS, and SnSe exhibit a combination of extraordinary properties: high carrier mobility, strong anisotropic, electronic, and optical properties that can be engineered by strain and controlled by external fields, and robust room-temperature ferroelectricity.[1−4] A large spontaneous ferroelectric polarization of ∼260−340 pC/m and the associated inversion symmetry breaking in monolayer GeSe are predicted to lead to extraordinarily large second-order electric susceptibilities responsible for nonlinear optical effects, such as optical second harmonic generation, optical rectification, and shift current.[4−8] A shift current is a zero-bias photocurrent resulting from a coherent spatial shift of the electron charge density in response to the excitation of an electron from the valence to the conduction band.[2,3,5,6,9−12] Pronounced nonlinear optical effects in the visible range that can be tuned by strain and external fields make monolayer GeSe and other group-IV monochalcogenides a promising platform for a variety of applications in lasers, electro-optic modulators, switches, and frequency conversion devices.[13] In particular, an efficient optical rectification and/or shift current response can give rise to emission of terahertz (THz) radiation in response to excitation with laser pulses of subpicosecond duration, putting GeSe forth as a candidate for THz sources for spectroscopy, imaging, and high-speed communication.[14,15] Furthermore, the shift current is a mechanism behind the bulk photovoltaic effect (BPVE).[3,6,12,16] BPVE-based GeSe solar cells may therefore provide an efficient alternative to traditional p−n junction-based ones.[16,17]

Although solution chemistry approaches and laser-assisted thinning show rapid progress toward the ultimate goal of reliable fabrication of large-area single-crystalline GeSe monolayers, no experimental studies of nonlinear optical properties of GeSe monolayers have been reported to date.[18,19] On the other hand, GeSe single crystals with dimensions in the millimeter range and larger can be reliably fabricated. Here, we present the first evidence of emission of THz pulses in response to above-bandgap photoexcitation of a bulk GeSe crystal with a thickness of approximately 100−200 μm and lateral dimensions of ∼2 mm. We attribute THz generation to the shift current response in the surface layer of GeSe.

Received: October 2, 2018
Accepted: January 8, 2019
Published: January 8, 2019

DOI: 10.1021/acsami.8b17225
ACS Appl. Mater. Interfaces 2019, 11, 5492−5498

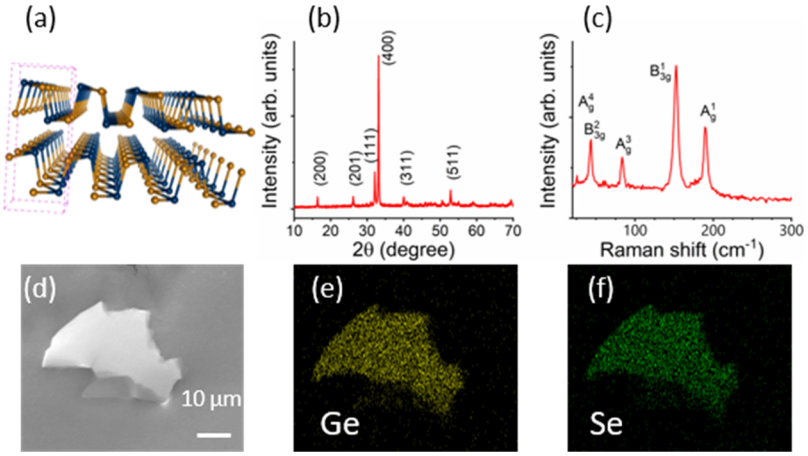

Figure 1. (a) Structural model of the GeSe crystal. Structural characterization: XRD (b) and bulk Raman spectroscopy (c) showing the orthorhombic crystal structure of GeSe crystal. (d) SEM image of a small GeSe flake mechanically exfoliated from the same bulk GeSe crystal as the one used in THz measurements, and the corresponding EDX maps showing the uniform distribution of Ge (e) and Se (f).

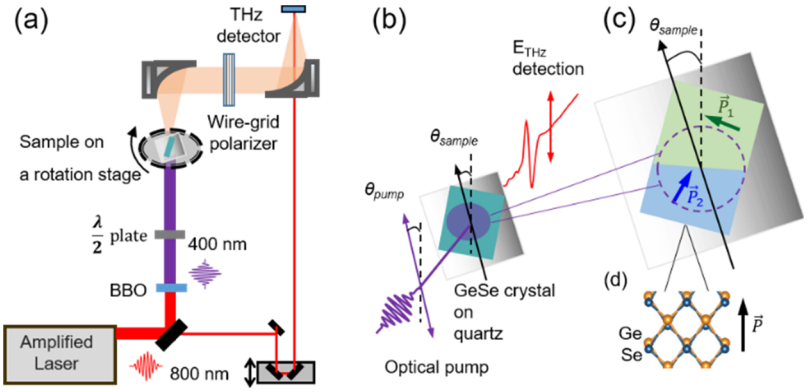

Figure 2. (a) Schematic diagram of the THz emission spectroscopy experiment. (b) Illustration of the experimental geometry where sample orientation and linear polarization of an optical pump pulse are varied relative to the fixed polarization of the detected THz pulses. (c) Schematic depiction of a GeSe crystal consisting of two crystal grains, each characterized by a spontaneous electric polarization vector along the armchair direction in the surface layer of GeSe (d).

Although the stacking sequence of the layers in this van der Waals material yields a centrosymmetric bulk structure that corresponds to the D_{2h} (*mmm*) point group (Figure 1a), inversion symmetry is broken at the surface and a spontaneous surface polarization can exist in the armchair direction just as it does in a monolayer GeSe.[7,9] Efficient THz generation has been previously reported in arrays of submicrometer-thick nanosheets of another group-IV monochalcogenide, GeS, and at that time was attributed either to a surface shift current or to emission from a small number of nanosheets with the low, odd number of layers with broken inversion symmetry.[3,20] Unlike the disordered array of GeS nanosheets, the present work focused on a macroscopic GeSe crystal, conclusively showing that THz generation in bulk-like group-IV monochalcogenides is a surface effect. Excitation fluence, orientation, and excitation polarization dependence of the THz emission confirm that shift currents flow along one crystallographic direction, presumably determined by the spontaneous polarization of the surface layer. Stronger THz emission in response to 400 nm excitation than to the comparable fluence of 800 nm excitation stems from stronger absorption of 400 nm light by GeSe, which leads to the higher excitation of a surface layer.[21] Highly efficient shift current photoexcitation in GeSe and the optical absorption that covers the entire visible range suggest applications of these layered materials in third-generation BPVE photovoltaics and nonlinear photonic devices. Finally, surface selectivity of THz emission may lead to new approaches to chemical sensing.

RESULTS AND DISCUSSION

We have used THz emission spectroscopy to study ultrafast dynamics of photoexcitation in a bulk GeSe crystal grown by chemical vapor transport. For measurements, a ∼100−200 μm thick crystal of ∼2 mm lateral dimensions was exfoliated from the as-grown bulk crystal using adhesive tape. In addition, other small exfoliated pieces from the same crystal were used for structural characterization (Figure 1b−f). THz emission spectroscopy allows electrical contact-free all-optical monitoring of transient real or polarization photocurrents by detecting, in the far field, THz radiation emitted by those currents.[11,20,22−27] We have performed THz emission measurements in transmission mode, with excitation and emission normal to the sample and therefore to the basal plane of the GeSe crystal, as illustrated schematically in Figure 2. Sample orientation was varied by rotation of a sample stage through an angle θ_{sample}, and the polarization of the optical pump pulse (θ_{pump}) was varied by a half-wave plate. We find that the photoexcited GeSe crystal emits nearly single-cycle THz pulses

DOI: 10.1021/acsami.8b17225
ACS Appl. Mater. Interfaces 2019, 11, 5492−5498

in response to either 800 (1.55 eV) or 400 nm (3.10 eV) excitation (Figure 3). With the linearly polarized excitation and

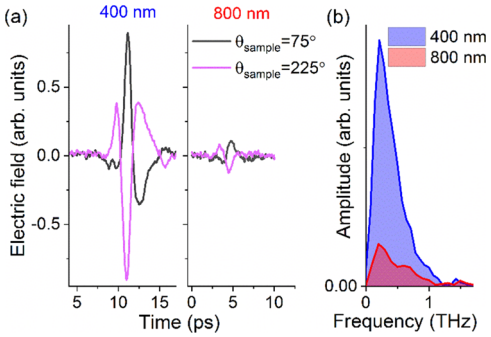

Figure 3. (a) THz waveforms emitted by the GeSe crystal as a result of excitation either with ~190 μJ/cm^2, 100 fs, 400 nm pulses (left panel) or with ~130 μJ/cm^2, 100 fs, 800 nm pulses (right panel), with θ_{pump} = 0° in both cases. Rotating the crystal by 180° reverses polarity of the emitted pulse. (b) Amplitude spectra of the THz waveforms excited with 400 and 800 nm pulses for θ_{sample} = 75°.

detection at normal incidence (Figure 2), we can only detect THz emission due to the real or polarization currents parallel to the crystal surface, ruling out the photo-Dember effect, photon drag, or emission due to drift of photoexcited carriers in built-in fields that are normal to the surface. In the absence of an external in-plane bias, possible mechanisms behind the observed THz emission involve second-order nonlinear processes. A single-color linearly polarized excitation precludes injection current. As both excitation energies are larger than ~1.2 eV band gap, real free carriers are excited and the shift current, associated with interband polarization, dominates over non-resonant optical rectification.[28−31] The observed THz emission thus indicates that above-bandgap excitation results in a shift current not only in GeSe monolayers, as has been predicted, but also in bulk GeSe crystals. Shift current resulting from excitation with ultrafast pulses gives rise to THz emission that varies as $\vec{E}_{shift} \propto \vec{J}_{shift}$ immediately above the GeSe surface and again reimaged onto the ZnTe detector crystal with the help of parabolic mirrors.[22,25,32]

A shift current is a second-order nonlinear effect and thus requires a broken inversion symmetry. In GeSe monolayers, inversion symmetry is broken by a spontaneous lattice strain and puckering, which results in a polar point group C_{2v} (*mm*2) symmetry and a concurrent large (260−340 pC/m) spontaneous polarization.[4−7] Inversion symmetry breaking is predicted to manifest in a pronounced zero-bias in-plane shift current upon above the bandgap photoexcitation.[3,5−8,10] Unlike the monolayers, bulk GeSe is characterized by the centrosymmetric D_{2h} (*mmm*) point group due to antiferroelectric stacking of consecutive layers (Figure 1a). However, inversion symmetry is broken at the surface, suggesting that the observed THz emission is due to a surface rather than a bulk shift current.

Analysis of the differences of THz emission following 400 and 800 nm excitation supports the surface origin of the observed THz emission. Assuming that the shift current in the top surface layer of a GeSe bulk crystal is qualitatively similar to that in a monolayer, shift current magnitude is expected to peak strongly immediately above the band gap and then fall off at higher energies.[5,6] As the optical penetration length of both 400 and 800 nm is significantly shorter than the thickness of the crystal,[21] the bottom surface does not contribute. We find that the spectrally integrated amplitude of the THz waveforms emitted following excitation with 800 nm (1.55 eV) is nearly 20% of that for 400 nm excitation (3.10 eV) (Figure 3b). Taking into account a ~30% difference in excitation fluence, 400 nm pulses result in ~3.5 times stronger emission for equivalent incident excitation fluence. However, the absorption coefficient is ~10-fold higher at 400 nm than 800 nm (~0.078 vs ~0.009 nm^{-1} at 800 nm).[21] Taking into account reflection losses (~47% for 400 nm and ~41% for 800 nm)[21] and using 0.25 nm as the thickness of a GeSe monolayer,[33] we calculate that equal incident excitation fluence results in ~7.7 times higher fluence or, equivalently, ~3.85 times higher number of photons absorbed in the topmost GeSe layer. Assuming that each absorbed photon promotes one electron from the valence to the conduction band, we find the contribution to the THz emission of each photon absorbed in the surface layer to be approximately equal regardless of its wavelength.

The amplitude of the observed THz emission peaks between 0.2 and 0.5 THz (Figure 3b). Temporal behavior of the shift current can be phenomenologically modeled as a convolution of the temporal derivative of the charge displacement with the pump intensity envelope.[22] For the pump pulse of ~100 fs duration, it is expected to vary on the subpicosecond timescale with the bandwidth of the emitted THz radiation extending to ~10 THz.[20,22] In the previous work on GeS nanosheets, we found that the bandwidth of the ZnTe detector crystal limited the observed bandwidth of THz emission.[20] However, in the case of GeSe, strong THz absorption by the sample itself is a limiting factor in uncovering the true ultrafast transient behavior of the surface shift currents from the THz pulses detected in the transmission geometry, as shown in the Supporting Information (Figure S1). The GeSe crystal absorbs over 80% of incident THz radiation that was generated in a 1 mm thick [110] ZnTe crystal, with absorbance increasing nearly fivefold from 0.2 to 1.8 THz. Strong THz absorption can be attributed to low-frequency B_{3u} and B_{1u} infrared-active phonons centered in the 2.5−2.6 THz range. B_{3u} phonons in particular are associated with the opposite motion of Ge and Se along the armchair direction and couple strongly to the THz radiation polarized along this direction. As a result, the GeSe crystal itself acts as a low-pass filter, attenuating THz pulses emitted by the surface layer and broadening them to 1−2 ps in duration, as shown in the Supporting Information (Figure S2). Reducing the GeSe thickness to minimize reabsorption of the emitted THz radiation would result in a broadband source with efficiency surpassing that of conventional sources, as illustrated in Figure S1.

Figure 3a also shows that rotating the sample by 180° while maintaining an unchanged pump polarization reverses the polarity of emission although the amplitude and temporal shape of the waveform show only a minimal change. This observation unequivocally shows that the inversion symmetry breaking in the surface layer of GeSe dictates the emission polarity and supports the surface shift current as a mechanism of THz generation.

Figure 4 provides a detailed analysis of THz emission dependence on sample orientation. Although the amplitude of the THz emission is nearly an order of magnitude lower for 800 nm excitation, the waveforms for the two excitation wavelengths are qualitatively the same for every sample orientation. As Figure 4a,d demonstrates, the observed waveform shape for both 400 and 800 nm excitation is well-

DOI: 10.1021/acsami.8b17225
ACS Appl. Mater. Interfaces 2019, 11, 5492−5498

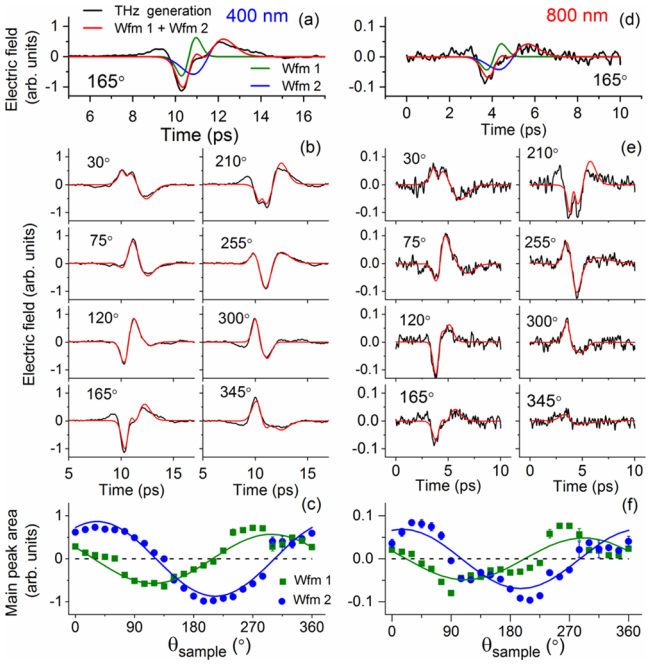

Figure 4. Dependence of THz emission excited with ~190 μJ/cm^2, 100 fs, 400 nm pulses (a–c) or with ~130 μJ/cm^2, 100 fs, 800 nm pulses (d–f), with θ_{pump} = 0° in both cases. (a) and (d) show examples of decomposition of the observed emission in two single-cycle transients, Wfm 1 and Wfm 2, corresponding to two crystal grains with different intrinsic surface polarizations in the excitation spot, as illustrated schematically in Figure 2c. (b) and (e) show emitted waveforms (black curves) and model fits to two transients (red curves) at different sample orientations. (c) and (f) show the area under the first peak of each of the two waveforms as a function of sample orientation. Symbols show the areas obtained from the best model fits to the observed THz transients, and solid lines represent the fit of the data to a cosine function.

described by a sum of two simple single-cycle bipolar Gaussian waveforms (e.g., the first derivatives of the Gaussian pulses, Figure S3). This decomposition of THz emission into two single-cycle transients at all sample orientations suggests the presence of two crystal grains within a 1.5 mm photoexcited area on the GeSe crystal, each characterized by a specific spontaneous polarization vector **P** that dictates the direction of the surface shift current. Figure 2c schematically illustrates the two grains as side-by-side as a result of a stacking fault; however, it is also possible that they fully or partially overlap or that they originate from a rotational misalignment between the GeSe layers within a crystal. Each of the two transients is bipolar, indicating that momentum relaxation time is shorter than the pump pulse duration and does not affect the emitted waveform shape in a significant way.[20,22] One of the single-cycle waveforms (Waveform 1: Wfm 1) has a Gaussian FWHM of 1.0 ± 0.3 ps. Another one (Waveform 2: Wfm 2) is delayed by 1.1 ± 0.2 ps and has a FWHM of 1.9 ± 0.6 ps. Delay in arrival time and longer duration of the second waveform indicate that the thickness of the crystal grain that emits Wfm 2 is larger. Figure 4b,c shows model fits to experimental THz waveforms excited by 400 and 800 nm pulses. Although simple Gaussian derivative pulses cannot account for a possible spectral chirp in each of the constituent pulses after propagation through the crystal, they adequately capture the sample orientation dependence of emitted THz waveforms. Figure 4c,f plots the area under each of the model single-cycle bipolar waveforms, with a sign that accounts for the polarity of the first peak of each waveform. For both waveforms, signed area follows a cosine dependence on the sample orientation. As we detect only one linearly polarized component of the emitted transient electric field, cosine dependence on sample orientation confirms that the shift current direction is determined by the intrinsic spontaneous surface polarization and associated inversion symmetry breaking of each crystalline grain. Shift current flows along the spontaneous polarization and emits electromagnetic radiation polarized along the direction of spontaneous polarization. Experimental waveforms represent a component of the emitted electromagnetic transient polarized along the detection axis. We find that for both 400 and 800 nm, Wfm 1 has a positive maximum when the sample is rotated by 68 ± 4° from the (arbitrarily chosen) origin, whereas Wfm 2 peaks at −30 ± 4°, with ~98° between the polarization directions in the two grains. Those angles indicate the direction of the photoexcited shift current in each of the grains.

The direction of the shift current, given by the spontaneous surface electric polarization, is presumed to be in a softer armchair direction of the GeSe lattice. We also expect the strong THz absorption due to the infrared-active low-frequency polar phonons to exhibit a significant dependence on the crystal orientation relative to the polarization of the incident THz radiation. The B_{3u} phonon in particular involves the motion of Ge and Se atoms in opposite directions along the armchair crystal direction and can therefore couple strongly to the THz radiation polarized along this direction. Indeed, such dependence exists. As shown in Figure 5, the

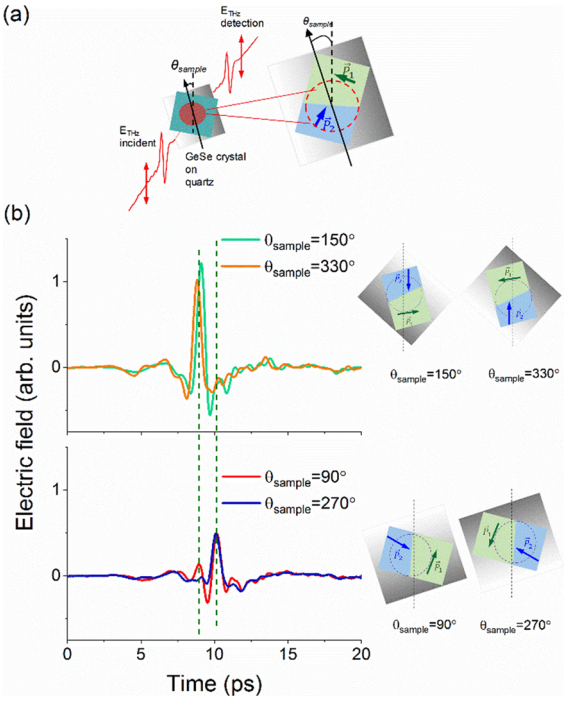

Figure 5. (a) Schematic diagram of the measurement of absorption of incident THz pulses generated in a ZnTe source by the GeSe crystal as a function of GeSe orientation. (b) Transmission of a THz pulse through two grains with different thicknesses and orientations splits the incident pulse into two. When polarization of the incident THz pulse has a large component parallel to the spontaneous electric polarization in a grain, its absorption is significantly stronger.

DOI: 10.1021/acsami.8b17225
ACS Appl. Mater. Interfaces 2019, 11, 5492–5498

incident THz pulse from a ZnTe source is not only strongly attenuated but also split into two pulses delayed by ~1.1 ps due to transmission through the two, a thinner and a thicker, grains in the 1.5 mm diameter THz spot size on the studied GeSe crystal (Figure 5a). Attenuation of the pulse transmitted through each grain is the strongest when it is polarized along the same direction as the THz pulses emitted by the GeSe surface layer. For θ_{sample} of 150 or 330°, spontaneous electric polarization of the thicker grain ($\mathbf{P_2}$) is approximately parallel to the incident THz polarization, and the second (delayed) peak is not present. At the same time, the polarization of the thinner grain has a large component that is perpendicular to the incident THz polarization, resulting in an incomplete attenuation of the first peak. We observe the opposite trends for sample orientations of 90 and 270°, where the first peak is almost fully attenuated while a small fraction of the second peak remains after propagation through the crystal. These results confirm that polarization of the THz pulses emitted by the surface shift current in GeSe coincides with the direction of the strongest attenuation by the infrared-active phonons, underscoring that thinner crystals will result in a much brighter THz source.

We also find that the amplitude, shape, and polarity of emitted THz waveforms are insensitive to the linear polarization of the pump pulse (Figure 6). Amplitude of the shift current can be expressed as

$$J_a = \frac{c\varepsilon_0}{2}\kappa^{abb}E_b(\omega)E_b(-\omega) \quad (1)$$

where J_a is the current in the a direction, $E_b(\omega)$ is the electric field of the optical excitation at frequency ω polarized in the b direction, κ^{abb} is the photoresponsivity tensor, c is the speed of light, and ε_0 is the permittivity of free space.[34] In GeSe, like in other ferroelectric group-IV monochalcogenides, shift current flows in the direction of polarization, and $J_a = J_x$, where x is the armchair direction.[6] Given a significant structural anisotropy of the crystal lattice structure between the armchair and zigzag directions, the observed independence of the shift current on pump polarization is unexpected. DFT calculation of κ^{xxx} and κ^{xyy} for a GeSe monolayer demonstrates that, although both functions have complicated and different energy dependence, there are multiple points along the energy axis where they cross, yielding a shift current that is independent of pump polarization. Our data show that this is the case for 400 nm (3.1 eV) excitation, and $\kappa^{xxx} = \kappa^{xyy}$ at this energy.

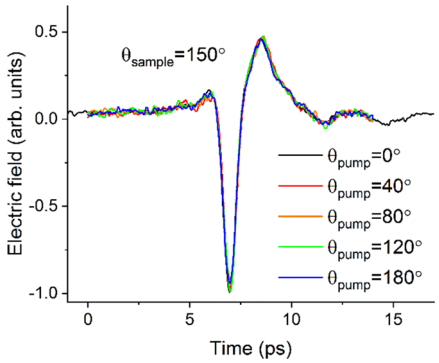

Figure 6. Selected THz waveforms excited by ~190 μJ/cm^2, 400 nm pulses with different pump linear polarization directions.

Finally, as eq 1 shows, we expect the shift current to depend linearly on excitation fluence. We find that increasing 400 nm excitation fluence increases the amplitude of the emitted THz waveforms but does not change the shape of the waveforms (Figure 7a) or the bandwidth of the emitted radiation (Figure 7b). The inset in Figure 7b shows the spectrally integrated electric field of THz pulses emitted by the GeSe crystal, which includes contributions of both crystalline grains present in the 1.5 mm diameter photoexcited area, and therefore, the transient shift current varies linearly in response to the excitation fluence.

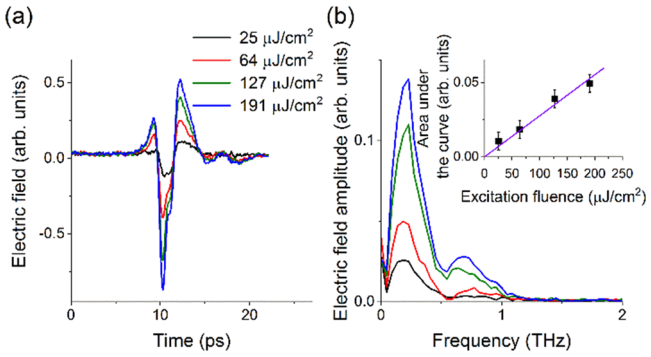

Figure 7. Excitation fluence dependence of THz generation in GeSe. (a) THz waveforms at different 400 nm photoexcitation fluence values. (b) The corresponding electric field spectral amplitude. Measurements were carried out with θ_{pump} = 0° and θ_{sample} = 180°.

CONCLUSIONS

In conclusion, we have presented the evidence of a surface shift current response in a bulk GeSe crystal. Although the stacking sequence of the layers in this van der Waals material results in the inversion symmetry in the bulk, this symmetry is broken at the surface. We find that photoexcited GeSe crystals emit nearly single-cycle THz pulses in response to either 800 (1.55 eV) or 400 nm (3.10 eV) excitation. Excitation fluence, sample orientation, and excitation polarization dependence of the THz emission confirm that shift current flowing along the spontaneous polarization of the surface layer is responsible for the observed emission. Stronger THz emission in response to 400 nm excitation compared to the comparable fluence of 800 nm excitation stems from the stronger absorption of 400 nm light by GeSe, which leads to the higher excitation of a surface layer. Highly efficient shift current in response to photoexcitation on both short- and long-wave edges of the visible spectrum suggests applications of these layered materials in solar cells based on BPVE photovoltaics. Efficient THz emission that is potentially tunable by strain can also be harnessed in new nonlinear photonic devices, sensors, and THz sources.

EXPERIMENTAL SECTION

GeSe Fabrication. GeSe single crystals were synthesized using chemical vapor transport growth using Ge (99.9999% purity) and Se (99.9999% purity) pieces. These precursors were mixed at atomic 50:50 ratios and sealed into 0.5 in. diameter and 9 in. long quartz tubes under 10^{-6} Torr pressure. Extra GeI_4 powder was added as a transport agent to initiate the crystal growth and successfully transport Ge and Se atomic species. Closely following Ge−Se binary phase diagrams, we have set the growth temperature at 550 °C and the cold temperature zone at 500 °C for 5 weeks to complete the growth.

DOI: 10.1021/acsami.8b17225
ACS Appl. Mater. Interfaces 2019, 11, 5492−5498

Samples were cooled down to room temperature, and ampoules were opened in a chemical glove box. Samples were characterized using XRD (Figure 1b), Raman spectroscopy (Figure 1c), SEM (Figure 1d), and EDS (Figure 1e,f).

THz Emission Spectroscopy. For THz emission spectroscopy measurements, a GeSe crystal with lateral dimensions of ∼2 mm was excited at normal incidence with either 400 or 800 nm, 100 fs laser pulses from a 1 kHz amplified Ti:Sapphire source, as illustrated schematically in Figure 2. The sample was placed behind a 1.5 mm diameter aperture (not shown) in the center of ∼7 mm diameter collimated excitation beam to ensure uniformity of excitation. The thickness of the samples is estimated to be on the order of 100−200 μm. A 1 mm thick fused quartz slide was placed over the crystal to fix it on the sample stage. A pair of off-axis parabolic mirrors focused the emitted THz pulses from the GeSe crystal within a 1.5 mm diameter photoexcited spot on a sample indicated by the circle in Figure 2 onto a [110] ZnTe crystal, where they were coherently detected by free-space electro-optic sampling.[14] The wire-grid polarizer (Microtech Instruments; field extinction ratio of 0.01) ensured that only a component of the generated THz pulses polarized in the direction, labeled as E_{THz} detection direction in Figure 2b, was detected. Sample orientation was varied by rotation of the sample stage through an angle θ_{sample}, and the polarization of the optical pump pulse (given by the angle of pump polarization relative to the vertical, θ_{pump}) was varied by a half-wave plate.

■ ASSOCIATED CONTENT

Supporting Information

The Supporting Information is available free of charge on the ACS Publications website at DOI: 10.1021/acsami.8b17225.

Illustration of the experimental geometry for measuring the THz absorbance of the GeSe crystal; waveforms of the THz pulse ; corresponding THz amplitude spectra; comparison of the amplitude spectra from ZnTe optical rectification source and GeSe crystal; effect of GeSe B_{3u} and other infrared-active phonons in the ∼2.5 THz spectral range, with the resulting waveforms; model single-cycle waveforms, with the direction of the current determined by spontaneous surface electric polarization (PDF)

■ AUTHOR INFORMATION

Corresponding Author

*E-mail: ltitova@wpi.edu.

ORCID

Sefaattin Tongay: 0000-0001-8294-984X

Lyubov V. Titova: 0000-0002-2146-9102

Notes

The authors declare no competing financial interest.

■ ACKNOWLEDGMENTS

We acknowledge support from the NSF DMR-1750944 (L.V.T.), NSF DMR-1552220 (S.T.), and NERSC-DOE DE-AC02-05CH11231 (B.M.F.).

■ REFERENCES

(1) Wu, M.; Zeng, X. C. Intrinsic Ferroelasticity and/or Multiferroicity in Two-Dimensional Phosphorene and Phosphorene Analogues. *Nano Lett.* **2016**, *16*, 3236−3241.

(2) Fei, R.; Kang, W.; Yang, L Ferroelectricity and Phase Transitions in Monolayer Group-Iv Monochalcogenides. *Phys. Rev. Lett.* **2016**, *117*, 097601.

(3) Cook, A. M.; Benjamin, M. F.; de Juan, F.; Coh, S.; Moore, J. E. Design Principles for Shift Current Photovoltaics. *Nat. Commun.* **2017**, *8*, 14176.

(4) Wang, H.; Qian, X. Two-Dimensional Multiferroics in Monolayer Group Iv Monochalcogenides. *2D Materials* **2017**, *4*, 015042.

(5) Panday, S. R.; Fregoso, B. M. Strong Second Harmonic Generation in Two-Dimensional Ferroelectric Iv-Monochalcogenides. *J. Phys.: Condens. Matter* **2017**, *29*, 43LT01.

(6) Rangel, T.; Fregoso, B. M.; Mendoza, B. S.; Morimoto, T.; Moore, J. E.; Neaton, J. B. Large Bulk Photovoltaic Effect and Spontaneous Polarization of Single-Layer Monochalcogenides. *Phys. Rev. Lett.* **2017**, *119*, 067402.

(7) Wang, H.; Qian, X. Giant Optical Second Harmonic Generation in Two-Dimensional Multiferroics. *Nano Lett.* **2017**, *17*, 5027−5034.

(8) Fregoso, B. M.; Morimoto, T.; Moore, J. E. Quantitative Relationship between Polarization Differences and the Zone-Averaged Shift Photocurrent. *Phys. Rev. B* **2017**, *96*, 075421.

(9) Fei, R.; Li, W.; Li, J.; Yang, L. Giant Piezoelectricity of Monolayer Group Iv Monochalcogenides: Snse, Sns, Gese, and Ges. *Appl. Phys. Lett.* **2015**, *107*, 173104.

(10) Mehboudi, M.; Fregoso, B. M.; Yang, Y.; Zhu, W.; van der Zande, A.; Ferrer, J.; Bellaiche, L.; Kumar, P.; Barraza-Lopez, S. Structural Phase Transition and Material Properties of Few-Layer Monochalcogenides. *Phys. Rev. Lett.* **2016**, *117*, 246802.

(11) Schleicher, J. M.; Harrel, S. M.; Schmuttenmaer, C. A. Effect of Spin-Polarized Electrons on Terahertz Emission from Photoexcited Gaas. *J. Appl. Phys.* **2009**, *105*, 113116.

(12) Ogawa, N.; Sotome, M.; Kaneko, Y.; Ogino, M.; Tokura, Y. Shift Current in the Ferroelectric Semiconductor Sbsi. *Phys. Rev. B* **2017**, *96*, 241203.

(13) Guan, S.; Liu, C.; Lu, Y.; Yao, Y.; Yang, S. A. Tunable Ferroelectricity and Anisotropic Electric Transport in Monolayer B-Gese. *Phys. Rev. B* **2018**, *97*, 144104.

(14) Jepsen, P. U.; Cooke, D. G.; Koch, M. Terahertz Spectroscopy and Imaging−Modern Techniques and Applications. *Laser Photonics Rev.* **2011**, *5*, 124−166.

(15) Tonouchi, M. Cutting-Edge Terahertz Technology. *Nat. Photonics* **2007**, *1*, 97−105.

(16) Butler, K. T.; Frost, J. M.; Walsh, A. Ferroelectric Materials for Solar Energy Conversion: Photoferroics Revisited. *Energy Environ. Sci.* **2015**, *8*, 838−848.

(17) Tan, L. Z.; Zheng, F.; Young, S. M.; Wang, F.; Liu, S.; Rappe, A. M. Shift Current Bulk Photovoltaic Effect in Polar Materials—Hybrid and Oxide Perovskites and Beyond. *npj Comput. Mater.* **2016**, *2*, 16026.

(18) Zhao, H.; Mao, Y.; Mao, X.; Shi, X.; Xu, C.; Wang, C.; Zhang, S.; Zhou, D. Band Structure and Photoelectric Characterization of Gese Monolayers. *Adv. Funct. Mater.* **2018**, *28*, 1704855.

(19) Ramasamy, P.; Kwak, D.; Lim, D.-H.; Ra, H.-S.; Lee, J.-S. Solution Synthesis of Ges and Gese Nanosheets for High-Sensitivity Photodetectors. *J. Mater. Chem. C* **2016**, *4*, 479−485.

(20) Kushnir, K.; Wang, M.; Fitzgerald, P. D.; Koski, K. J.; Titova, L. V. Ultrafast Zero-Bias Photocurrent in Ges Nanosheets: Promise for Photovoltaics. *ACS Energy Lett.* **2017**, 1429−1434.

(21) Liu, S.-C.; Mi, Y.; Xue, D.-J.; Chen, Y.-X.; He, C.; Liu, X.; Hu, J.-S.; Wan, L.-J. Investigation of Physical and Electronic Properties of Gese for Photovoltaic Applications. *Adv. Electron. Mater.* **2017**, *3*, 1700141.

(22) Braun, L.; Mussler, G.; Hruban, A.; Konczykowski, M.; Schumann, T.; Wolf, M.; Münzenberg, M.; Perfetti, L.; Kampfrath, T. Ultrafast Photocurrents at the Surface of the Three-Dimensional Topological Insulator Bi_2Se_3. *Nat. Commun.* **2016**, *7*, 13259.

(23) Bieler, M.; Pierz, K.; Siegner, U.; Dawson, P. Shift Currents from Symmetry Reduction and Coulomb Effects in (110)-Orientated Gaas\$Al_{0.3}ga_{0.7}$as Quantum Wells. *Phys. Rev. B* **2007**, *76*, 161304.

(24) Laman, N.; Bieler, M.; van Driel, H. M. Ultrafast Shift and Injection Currents Observed in Wurtzite Semiconductors Via Emitted Terahertz Radiation. *J. Appl. Phys.* **2005**, *98*, 103507.

(25) Priyadarshi, S.; Leidinger, M.; Pierz, K.; Racu, A. M.; Siegner, U.; Bieler, M.; Dawson, P. Terahertz Spectroscopy of Shift Currents

DOI: 10.1021/acsami.8b17225
ACS Appl. Mater. Interfaces 2019, 11, 5492−5498

Resulting from Asymmetric (110)-Oriented Gaas/Algaas Quantum Wells. *Appl. Phys. Lett.* **2009**, *95*, 151110.
(26) Titova, L. V.; Pint, C. L.; Zhang, Q.; Hauge, R. H.; Kono, J.; Hegmann, F. A. Generation of Terahertz Radiation by Optical Excitation of Aligned Carbon Nanotubes. *Nano Lett.* **2015**, *15*, 3267−3272.
(27) Bagsican, F. R.; Zhang, X.; Ma, L.; Wang, M.; Murakami, H.; Vajtai, R.; Ajayan, P. M.; Kono, J.; Tonouchi, M.; Kawayama, I. Effect of Oxygen Adsorbates on Terahertz Emission Properties of Various Semiconductor Surfaces Covered with Graphene. *J. Infrared, Millimeter, Terahertz Waves* **2016**, *37*, 1117−1123.
(28) Nastos, F.; Sipe, J. E. Optical Rectification and Shift Currents in Gaas and Gap Response: Below and above the Band Gap. *Phys. Rev. B* **2006**, *74*, 035201.
(29) Côté, D.; Laman, N.; van Driel, H. M. Rectification and Shift Currents in Gaas. *Appl. Phys. Lett.* **2002**, *80*, 905−907.
(30) Bieler, M Thz Generation from Resonant Excitation of Semiconductor Nanostructures: Investigation of Second-Order Nonlinear Optical Effects. *IEEE J. Sel. Top. Quantum Electron.* **2008**, *14*, 458−469.
(31) Sipe, J. E.; Shkrebtii, A. I. Second-Order Optical Response in Semiconductors. *Phys. Rev. B* **2000**, *61*, 5337−5352.
(32) Côté, D.; Sipe, J. E.; van Driel, H. M. Simple Method for Calculating the Propagation of Terahertz Radiation in Experimental Geometries. *J. Opt. Soc. Am. B* **2003**, *20*, 1374−1385.
(33) Mounet, N.; Gibertini, M.; Schwaller, P.; Campi, D.; Merkys, A.; Marrazzo, A.; Sohier, T.; Castelli, I. E.; Cepellotti, A.; Pizzi, G.; Marzari, N. Two-Dimensional Materials from High-Throughput Computational Exfoliation of Experimentally Known Compounds. *Nat. Nanotechnol.* **2018**, *13*, 246−252.
(34) Young, S. M.; Rappe, A. M First Principles Calculation of the Shift Current Photovoltaic Effect in Ferroelectrics. *Phys. Rev. Lett.* **2012**, *109*, 116601.

DOI: 10.1021/acsami.8b17225
ACS Appl. Mater. Interfaces 2019, 11, 5492−5498